Authors' copy, as published in:

Composites Science and Technology, Volume 114, 19 June 2015, Pages 103–109.

http://dx.doi.org/10.1016/j.compscitech.2015.04.012

Effect of interfacial interactions on the electromechanical response of poly(vinylidene fluoride-trifluoroethylene)/$BaTiO_3$ composites and its time dependence after poling

Sara Dalle Vacche[a], Yves Leterrier[a,*], Véronique Michaud[a], Dragan Damjanovic[b], Arthur B. Aebersold [a,1], Jan-Anders E. Månson[a]

[a] Laboratoire de Technologie des Composites et Polymères (LTC), Ecole Polytechnique Fédérale de Lausanne (EPFL), CH-1015 Lausanne, Switzerland

[b] Ceramics Laboratory (LC), Ecole Polytechnique Fédérale de Lausanne (EPFL), CH-1015 Lausanne, Switzerland

[*] Corresponding author: Tel: + 41 21 6934848, Fax: + 41 21 6935880, E-mail : yves.leterrier@epfl.ch , Address: EPFL-STI-IMX-LTC, Station 12, CH-1015 Lausanne, Switzerland

Abstract

Solvent cast and compression molded composite films based on poly(vinylidene fluoride-trifluoroethylene), containing pristine and silylated $BaTiO_3$ particles, were poled, and their electromechanical response (d_{33}), their dielectric properties, and the crystalline structure of the embedded $BaTiO_3$ particles, probed by X-ray diffraction, were recorded during one week. Their d_{33} was also measured after long-term aging (>3years). During this time the d_{33} decreased for all composites. The d_{33} of solvent cast

[1] Current address: Interdisciplinary Center for Electron Microscopy (CIME), Ecole Polytechnique Fédérale de Lausanne (EPFL) , CH-1015 Lausanne, Switzerland

composites was higher when surface modified particles were used, both immediately after poling and after aging, while for compression molded composites only slight differences in the initial and aged d_{33} of materials containing pristine *versus* modified particles were found. However the decay rate of d_{33} in the short time after poling was highly affected by the surface modification of the particles for both the solvent cast and the compression molded composites. The results suggest that other phenomena besides the polarization of the ceramic particles and of the polymer matrix contribute to the measured electromechanical response of the composites. Charge accumulation and differences in the charge distribution due to the presence of the silane layer on the surface of $BaTiO_3$ may play an important role.

Keywords

A. Coupling agents A. Functional composites A. Polymer-matrix composites (PMCs) B. Electrical properties

1. Introduction

Since the discovery of the piezoelectric, pyroelectric, and ferroelectric properties of poly(vinylidene fluoride) (PVDF) [1-3], polymers and copolymers based on vinylidene fluoride (VDF) have been investigated for a wide range of applications, including actuators, detectors, transducers and energy converters [4-6]. The ferroelectric properties of VDF (co)polymers can be enhanced or tailored with the addition of fillers. The ferroelectric β-phase of PVDF, usually obtained by stretching, was nucleated by fillers, as e.g. $BaTiO_3$ [7] or carbon nanotubes [8], and the d_{33} of PVDF doubled upon addition of small quantities of carbon fullerenes and single-walled carbon nanotubes [9]. When the filler is a ferroelectric ceramic, interesting opportunities open up for the fabrication of composites with tuned pyroelectric and piezoelectric properties [10-12]. The possibility to use poly(vinylidene fluoride-trifluoroethylene) (P(VDF-TrFE))/ZnO

transducers for active sensing and damage detection has also been demonstrated [13]. VDF (co)polymers require relatively high electrical fields of more than 500 kV/cm for complete poling. By introducing high volume fractions of piezoelectric ceramic fillers, as e.g PZT ($Pb(Zr,Ti)O_3$) or $BaTiO_3$, in a VDF (co)polymer matrix, it is possible to obtain a piezoelectric response similar to that of the unfilled polymer with a lower applied electrical field, sufficient for poling the ceramic inclusions [14]. However, the fabrication of these composites is challenging due to the high surface energy difference between the polymer matrix and the inorganic filler. Particle agglomeration and porosity become important and hinder the mechanical, dielectric and piezoelectric properties at high filler volume fractions [15]. To overcome these issues, different approaches were developed, based on the modification of the matrix-filler interfacial interactions, either by introducing functional groups at the filler's surface [16], or by grafting bridging groups onto the polymer chains [17]. Surface modification of PZT particles allowed fabricating epoxy/PZT composites with enhanced piezoelectric properties, by improving the homogeneity of the film and reducing the electric field distortion during poling [18]. Another important characteristic for real-life applications is the stability of the electromechanical response with time. The d_{33} of PVDF was found to be stable in time at room temperature and to decrease with logarithmic kinetics at temperatures above 70 °C [19]; for piezoelectric ceramics the decay rate of d_{33} is of the order of few percent per time decade both at room temperature and at 250 °C [20, 21]. Few studies describe the time evolution of the piezoelectric coefficient of polymer-ceramic composites, and the observed behaviors do not always agree. The d_{33} of 3-1 epoxy/PZT composites was found to decrease in time with logarithmic kinetics; the decay rate was similar to that of PZT alone at high ceramic volume fractions, and higher for low ceramic volume fraction composites having higher ceramic surface to volume

ratio [21]. Similarly, a logarithmic decay with time was reported for the d_{33} of laminated PVDF-PMMA/$BaTiO_3$-PMMA composites [22]. On the other hand the hydrostatic piezoelectric response of 3-0 epoxy/$Sn_2P_2S_6$ composites was found to increase with time, and this effect was ascribed to the screening of spontaneous polarization in the ferroelectric particles [23]. To date, systematic studies on the time dependency of the electromechanical response of polymer-ceramic composites are missing. In previous work we reported that the d_{33} of P(VDF-TrFE)/$BaTiO_3$ composites decayed after poling; the decay rate was found to depend on the type and the volume fraction of the particles [15]. In parallel, we showed that composites produced using $BaTiO_3$ particles surface modified with (3-aminopropyl) triethoxysilane had lower porosity and improved mechanical and dielectric properties with respect to those produced with pristine particles [16]. In the present work, we focus on the effect of surface modification of $BaTiO_3$ on the piezoelectric response of P(VDF-TrFE)/$BaTiO_3$ composites, and on its evolution during one week after poling. To better understand long-term aging behavior, the study also includes data taken three years after poling.

2. Materials and methods

P(VDF-TrFE) (77/23 mol%) in powder form was provided by Solvay Solexis SpA (Bollate, MI, Italy). Three $BaTiO_3$ powders were used as piezoelectric ceramic fillers. BT1 was barium titanate (IV), <2 μm, 99.9 % (Sigma-Aldrich, MO, USA), average particle size 1.1 μm [15], BT2 was an in-house made $BaTiO_3$ powder with average particle size of 0.7 μm [15], and BT3 was $BaTiO_3$, 99.95 %, electronic grade (Inframat Advanced Materials LLC CT, USA) with a declared average particle size of 0.2 μm. The $BaTiO_3$ powders were surface modified with APTES ((3-aminopropyl) triethoxysilane, 99 %, Sigma-Aldrich, St. Louis, MO, USA) in ethanol/water (95/5 vol%). Composites containing 60 vol% (83 wt%) of $BaTiO_3$ were produced by casting

films using 2-butanone as a solvent, drying in a vacuum oven at 80 °C and annealing at 135 °C (SC films). Parts of these films were then compression molded (CM films). More information about the materials and procedures is reported in previous work [15, 16]. Composites made with untreated particles were named SC*x* and CM*x*, while those containing silylated particles were named SC*x*-APTES and CM*x*-APTES, where *x* is 1, 2, 3 for BT1, BT2 and BT3, respectively. For reference, unfilled P(VDF-TrFE) films were obtained with the same procedures, and were named SC0 and CM0.

Gold electrodes were deposited by sputtering on both sides of the films, and 5x5 mm^2 specimens were cut for the characterization. Before poling, the relative permittivity, ε_r, and the dielectric loss tangent, $\tan\delta_{diel}$, were measured, and the crystal structure of the embedded $BaTiO_3$ was assessed by X-ray diffraction (XRD). Then the specimens were poled in silicon oil, applying an electric field of 100 kV/cm for 30 minutes at 110 °C plus 30 minutes cooling to 35 °C. The piezoelectric coefficient, d_{33}, the relative permittivity, and the dielectric loss tangent were measured at room temperature within 15 minutes from poling, and XRD was performed within one hour. The measurements were then regularly repeated during one week; d_{33} was also measured after long-term aging at ambient conditions (after about 33'000 hours). The d_{33} was measured with an in-house made Berlincourt-type d_{33}-meter. Capacitance and dielectric loss tangent were measured with an impedance/gain-phase analyzer HP4194A (Hewlett Packard, USA) at room temperature between 10^2 and 10^6 Hz with a voltage of 1 V_{rms}. Relative permittivity was calculated from capacitance knowing the electrode area and the thickness of the specimens. From the ε_r curves of poled samples, where resonance peaks appeared, the resonance frequency *f* was monitored, which is linked to the stiffness of the material by the relationship $f \propto (1/h)\sqrt{(E/\rho)}$, where *h* is the linear dimension of the specimen that determines the resonance frequency, ρ its density and *E* its effective

elastic modulus [24]. XRD was performed with a D8 DISCOVER diffractometer (Bruker AXS, USA) with CuKα radiation. The polarization degree of the $BaTiO_3$ particles was inferred from the ratio ($I_{(002)}/I_{(200)}$) of the intensities of the peaks corresponding to the (002) and (200) planes of $BaTiO_3$, appearing at 2θ angles of 44.9 and 45.4 degrees, respectively.

3. Results

3.1 Solvent cast and compression molded unfilled P(VDF-TrFE) films

Unfilled P(VDF-TrFE) films were poled applying the same poling conditions as for the composites. The poling field, 100 kV/cm, was lower than what is usually applied for poling P(VDF-TrFE). The material was thus not fully poled, and therefore the piezoelectric coefficients d_{33} measured for the unfilled polymer films, shown in figure 1, were lower than expected for P(VDF-TrFE). The d_{33} values were stable in the observed 1-week time for both SC and CM films. As shown in figure 2, the relative permittivity of the P(VDF-TrFE) films increased upon poling, possibly due to the alignment of dipoles in the piezoelectric phase [25], and then slowly decreased with time after poling. The dielectric loss tangent also slightly increased upon poling and then decreased with time. Resonance peaks, magnified in the insets of figure 2, appeared on the relative permittivity and loss tangent patterns of poled specimens, with small amplitude. Their resonance frequency (~1.4×10^5 Hz) and amplitude did not appreciably change in the observed time, which is consistent with stable mechanical modulus and piezoelectric coefficient [26].

3.2 Solvent cast composites

The d_{33} of the SC composites made with untreated and silylated BT1 and BT2 is shown in figure 3. During poling of the SC2 specimens some punctual breakdown events occurred, probably due to a high current discharge through internal paths with higher

conductivity. These events, however, did not prevent completing the poling procedure, as the samples immediately recovered, possibly because the conductive path melted and the current stopped flowing through, and the electrical field could be applied again.
For all SC composites, the d_{33} decreased with time elapsed from poling. Immediately after poling the d_{33} values measured for the composites made with silylated powders (d_{33} > 20 pC/N) were twice as high as for the composites made with untreated powders (about 10 pC/N). After one week the d_{33} of the composites made with pristine powders had reached a plateau value at 4-5 pC/N. This was not the case for composites made with silylated powders, which showed d_{33} values of 7-10 pC/N. After long-term aging the difference between the d_{33} values of composites made with pristine *versus* silylated powders continued to decrease, with still slightly higher values measured for the latter.
Before poling, the relative permittivity of the SC composites containing pristine particles was lower than that of those containing modified particles. The permittivity of the SC1, SC1-APTES and SC2-APTES composites decreased by 5-15 % upon poling and then remained fairly stable in time, as shown in figure 4. The SC2 composites showed a larger decrease of permittivity upon poling, attributed to the mentioned breakdown events. Resonance peaks were visible at about 10^5 Hz for the poled composites made with treated BT1 and BT2, while they could not be clearly identified for the composites made with untreated powders. The amplitude of the resonance peaks decreased with time after poling, while the resonance frequency remained constant.
XRD after poling was only performed on the samples made with pristine and APTES treated BT2 (figure 5). About 10 minutes after poling SC2-APTES showed a higher $I_{(002)}/I_{(200)}$ than SC2, indicating better poling of $BaTiO_3$, and in the time that followed the $I_{(002)}/I_{(200)}$ ratio slightly decreased for both composites.

3.3 Compression molded composites

The piezoelectric coefficients of CM composites are shown in figure 6. The initial d_{33} of CM1 and CM1-APTES were similar, although CM1 showed a larger specimen-to-specimen variability, probably due to a lower macroscopic homogeneity of the composite. The CM2 specimens and some of the CM3 specimens suffered from punctual breakdown events during poling, as described for the solvent cast composites. The values of d_{33} measured for CM2-APTES and CM3-APTES right after poling were 15-20 % higher than for composites made with the corresponding pristine particles. For composites made with pristine powders d_{33} decayed very rapidly during the first few hours after poling, therefore the measured value of d_{33} was highly dependent on the time elapsed; as a result, some uncertainty is expected for the reported values at short time from poling. After about 5 hours the decay rate of d_{33} became much lower, and after one week the measured d_{33} values were about 8 pC/N for CM1 and CM3, and 5-6 pC/N for CM2. The decay rate of d_{33} was constant for the composites made with modified powders until the end of the first week, when they showed d_{33} values of about 10 pC/N. After long term aging no significant difference for d_{33} could be detected between CM1 and CM1-APTES (7 pC/N) and between CM3 and CM3-APTES (8 pC/N). Long term aged CM2-APTES had a d_{33} of 6 pC/N, similar to that of CM2 after 1 week (no long term aging was possible for CM2 as the specimens were very brittle and broke after few measurements). Upon poling the permittivity of all composites decreased, then increased again during few hours, until a stable value was reached, lower than that of the unpoled state (figure 7). At 5×10^5 Hz, the decrease of ε_r upon poling was found to be generally of 10–20 %, and larger for the specimens that suffered from breakdown events. As the materials made with untreated particles were brittle, small parts of the specimens broke during the measurements, leading to some uncertainty on the estimation of their area and hence on the calculation of ε_r. The relative permittivity and

dielectric loss tangent of CM composites as function of frequency, before poling and in time after poling, are shown in figure 8. After poling resonance peaks were identified on the ε_r and $\tan\delta_{diel}$ patterns around $2x10^5$ Hz. The resonance frequency remained constant in time for each specimen, while the amplitude of the resonance peaks decreased. The amplitude of the resonance peaks was similar for CM1 and CM1-APTES 5 minutes after poling, but decreased faster for CM1. For CM2 and CM3 the amplitude was lower than for CM2-APTES and CM3-APTES since the first measurements, taken within the first hour from poling; for CM2 the resonance peak was difficult to identify even 10 minutes after poling. The XRD analysis of the CM composites before and after poling (figure 9) highlighted that two time windows should be considered: (i) up to few hours after poling and (ii) after longer elapsed times. For all materials, after few hours from poling $I_{(002)}/I_{(200)}$ decreased with time. At the longer times, when comparing pairs of composites containing the same $BaTiO_3$ particles, pristine and modified, the differences observed for the $I_{(002)}/I_{(200)}$ ratio matched those observed for d_{33}. As an example, one day after poling CM1 had lower d_{33} and $I_{(002)}/I_{(200)}$ ratio (inset of figure 9) than CM1-APTES, while CM3 had similar d_{33} and $I_{(002)}/I_{(200)}$ ratio to CM3-APTES. Unexpectedly, for most of the CM materials the evolution of the (002) and (200) peaks during the first hours after poling did not match the evolution of d_{33}, and the $I_{(002)}/I_{(200)}$ ratio increased while the poling electric field had already been removed. Unfortunately, due to the duration of one XRD scan, long compared to the time scale of the phenomenon observed, it was not possible to perform enough measurements in this short time period to clearly elucidate this phenomenon. Again, the results at short times after poling were highly dependent on the time elapsed, which makes a side-by-side comparison of the unmodified *versus* modified materials difficult to perform.

4. Discussion

The higher d_{33} shown by the SC composites made with modified *versus* pristine particles in the entire time range was in line with their higher permittivity, attributed to their lower porosity [16], which may allow more effective poling. On the other hand, the d_{33} of CM composites made with either pristine or silylated $BaTiO_3$ were not significantly different after long-term aging. Interestingly, for both SC and CM composites a clear difference was shown for the decay kinetics of the d_{33} when pristine *versus* silylated particles were used. A widely used equation for describing the aging of the dielectric and piezoelectric properties is:

$$\frac{p_2 - p_1}{p_1} = k \, log \frac{t_2}{t_1} \qquad (1)$$

where p_i is the value of the studied property at the time t_i, and k is the aging rate [27]. In an initial period, which duration ranged from less than 1 hour to more than 1 week, the d_{33} of all the studied composites decreased at a greater rate than typically reported for aging of PVDF and piezoelectric ceramics taken separately. When pristine particles were used the d_{33} decayed very rapidly in the initial 30 minutes for SC composites, and in the first 1-5 hours for CM composites. For the former using equation 1 to describe the decay of the d_{33} in the initial period was not possible, while for the latter it would lead to k values of about -0.3, although this value has a large error due to the small number and to the large scatter of the experimental data collected in that timeframe. For the SC and CM composites made with silylated particles, the d_{33} decreased at a fairly constant rate during the first week, and fitting of the d_{33} *versus* time data with equation 1 (dashed lines in figures 3 and 6) in that timeframe led to values of k between -0.18 and -0.16 ($R^2 > 0.94$). For all composites the d_{33} data collected at long term suggest that after the initial fast decay period the decay rate became one order of magnitude lower, although a good fit with equation 1 was not possible.

The permittivity decrease observed for all composites upon poling was consistent with

the decrease of permittivity of $BaTiO_3$ particles due to the de-alignment of domains from the poling direction. The increase of permittivity and the decrease of the amplitude of the resonance peaks with time after poling, as well as the decrease of the $I_{(002)}/I_{(200)}$ ratio at long times after poling were consistent with a loss of polarization of the $BaTiO_3$ particles. It is worth noting, though, that the poling process is similar to that used for charging electrets. As these composites have some porosity and interfacial defects, electromechanical response due to electret effect might appear in addition to the piezoelectric response due to the poling of $BaTiO_3$ particles. Indeed, the composites made with pristine particles showed a marked Maxwell Wagner Sillars (MWS) effect before poling, due to space charges, with permittivity and losses increasing at low frequencies [28]. Upon poling this effect was initially suppressed, indicating that the charges were trapped, and then increased as charges diffused away from trapping centers. MWS effect was not observed with silylated particles, suggesting a modification of the space charge distribution due to the presence of the silane layer [29]. Thus the initial electromechanical response could include an electret contribution due to charge trapping. In the initial time window the charge would become free again and the electret effect would disappear [30], quite rapidly for composites made with pristine particles, and more slowly for composites made with silylated particles. At longer times only the piezoelectric effect due to poling of $BaTiO_3$ would remain, and the residual d_{33} decay would reflect a depolarization of the ceramic particles during aging.

At this stage, discriminating between the depoling effects due to release of trapped charges and aging of ferroelectric particles is not possible; further experiments are ongoing to elucidate the mechanisms governing the electromechanical response of these composites. Thermally stimulated current measurements (not shown here) were performed to reveal thermally activated release of trapped charges. However it was not

possible to observe charge de-trapping, because either electret depolarization was masked by the large depolarization peaks of P(VDF-TrFE) and $BaTiO_3$ appearing close to their Curie temperatures (127 °C and 130 °C, respectively), the energy of trapping was such to lead to electret depolarization above the melting temperature of the polymer (145 °C), or concentration of trapped charges was too small.

5. Conclusions

Surface modification of the $BaTiO_3$ particles with aminosilane led to a higher piezoelectric coefficient for solvent cast composite films, attributed to a better polarization of $BaTiO_3$. Different decay kinetics of the piezoelectric coefficient with time after poling were observed for both solvent cast and compression molded composites made with pristine *versus* modified particles. In addition to the polarization of the ceramic particles and of the polymer matrix, other effects, such as the formation of electrets or space charges, which may also be influenced by the poling conditions, are suspected to contribute to the rapid decay of the piezoelectric response of the composites after poling. Characteristic times span from only few hours in the case of composites made with pristine $BaTiO_3$ to more than one week when modified powders were used. It is thus recommended, when studying the electromechanical response of polymer-ceramic composites, to take into account that the time needed to achieve a stable d_{33}value after poling may differ depending on the properties of the polymer-ceramic interface and on the poling conditions, and to adapt the measurement protocol accordingly.

Acknowledgements

The authors would like to thank the Swiss National Science Foundation for funding in the framework of the Marie Heim-Vögtlin program, Solvay Solexis SpA for kindly providing P(VDF-TrFE), and Dr Li Jin and Mr Felix Lindström for technical support.

References

[1] Kawai H. Piezoelectricity of poly (vinylidene fluoride). Japanese Journal of Applied Physics. 1969;8(7):975-976.

[2] Bergman JG, McFee JH, Crane GR. Pyroelectricity and optical second harmonic generation in polyvinylidene fluoride films. Applied Physics Letters. 1971;18(5):203-205.

[3] Kepler RG, Anderson RA. Ferroelectricity in polyvinylidene fluoride. Journal of Applied Physics. 1978;49(3):1232-1235.

[4] Seo I, Zou D. Electromechanical Applications. In: Nalwa HS, editor. Ferroelectric polymers: chemistry, physics, and applications, New York: Marcel Dekker, Inc.; 1995. p. 699-734.

[5] Nguyen H, Navid A, Pilon L. Pyroelectric energy converter using co-polymer P(VDF-TrFE) and Olsen cycle for waste heat energy harvesting. Applied Thermal Engineering. 2010;30(14–15):2127-2137.

[6] Lang SB, Muensit S. Review of some lesser-known applications of piezoelectric and pyroelectric polymers. Applied Physics A-Materials Science & Processing. 2006;85(2):125-134.

[7] Mendes SF, Costa CM, Caparros C, Sencadas V, Lanceros-Mendez S. Effect of filler size and concentration on the structure and properties of poly(vinylidene fluoride)/$BaTiO_3$ nanocomposites. Journal of Materials Science. 2012;47(3):1378-1388.

[8] Lund A, Gustafsson C, Bertilsson H, Rychwalski RW. Enhancement of β phase crystals formation with the use of nanofillers in PVDF films and fibres. Composites Science and Technology. 2011;71(2):222-229.

[9] Baur C, DiMaio JR, McAllister E, Hossini R, Wagener E, Ballato J, et al. Enhanced piezoelectric performance from carbon fluoropolymer nanocomposites. Journal of

Applied Physics. 2012;112(12):124104.

[10] Ploss B, Ng W-Y, Chan HL-W, Ploss B, Choy C-L. Poling study of PZT/P(VDF-TrFE) composites. Composites Science and Technology. 2001;61(7):957-962.

[11] Ploss B, Shin FG, Chan HLW, Choy CL. Pyroelectric activity of ferroelectric PT/PVDF-TRFE. IEEE Transactions on Dielectrics and Electrical Insulation. 2000;7(4):517-522.

[12] Dietze M, Krause J, Solterbeck CH, Es-Souni M. Thick film polymer-ceramic composites for pyroelectric applications. Journal of Applied Physics. 2007;101(5): 054113.

[13] Meyers FN, Loh KJ, Dodds JS, Baltazar A. Active sensing and damage detection using piezoelectric zinc oxide-based nanocomposites. Nanotechnology.2013;24:185501.

[14] Babu I, de With G. Highly flexible piezoelectric 0-3 PZT-PDMS composites with high filler content. Composites Science and Technology. 2014;91:91-97.

[15] Dalle Vacche S, Oliveira F, Leterrier Y, Michaud V, Damjanovic D, Manson JAE. The effect of processing conditions on the morphology, thermomechanical, dielectric, and piezoelectric properties of P(VDF-TrFE)/$BaTiO_3$ composites. Journal of Materials Science. 2012;47(11):4763-4774.

[16] Dalle Vacche S, Oliveira F, Leterrier Y, Michaud V, Damjanovic D, Månson J-A. Effect of silane coupling agent on the morphology, structure, and properties of poly(vinylidene fluoride–trifluoroethylene)/$BaTiO_3$ composites. Journal of Materials Science. 2014;49(13):4552-4564.

[17] Lin MF, Lee PS. Formation of PVDF-g-HEMA/$BaTiO_3$ nanocomposites via in situ nanoparticle synthesis for high performance capacitor applications. Journal of Materials Chemistry A. 2013;1(46):14455-14459.

[18] Saber N, Ma J, Hsu HY, Lee SH, Marney D. Effect of surface modification of lead

zirconate titanate particles on the properties of piezoelectric composite sensors. In: Epaarachchi JA, Lau AKT, Leng J, editors. Fourth International Conference on Smart Materials and Nanotechnology in Engineering. Bellingham: SPIE; 2013.

[19] Kolbeck AG. Aging of piezoelectricity in poly(vinylidene fluoride). Journal of Polymer Science Part B-Polymer Physics. 1982;20(11):1987-2001.

[20] Gotmare SW, Leontsev SO, Eitel RE. Thermal degradation and aging of high-temperature piezoelectric ceramics. Journal of the American Ceramics Society 2010;93(7):1965-1969.

[21] Barzegar A, Bagheri R, Taheri AK. Aging of piezoelectric composite transducers. Journal of Applied Physics. 2001;89(4):2322-2326.

[22] Mazur K. Piezoelectricity of PVDF/ PUE, PVDF /PMMA and PVDF/ (PMMA+$BaTiO_3$) laminates. Proceedings of the 7th international symposium on electrets (ISE 7), p. 512-517. New York: IEEE; 1991.

[23] Maior MM, Prits IP, Vysochanskii YM. Screening of ferroelectric polarization and stability of poled state in $Sn_2P_2S_6$/epoxy composites. Ferroelectrics. 2002;281:35-40.

[24] IRE standards on piezoelectric crystals - determination of the elastic, piezoelectric, and dielectric constants - the electromechanical coupling factor, 1958. Proceedings of the Institute of Radio Engineers, vol. 461958. p. 764-778.

[25] Sencadas V, Costa CM, Moreira V, Monteiro J, Mendiratta SK, Mano JF, et al. Poling of beta-poly(vinylidene fluoride): dielectric and IR spectroscopy studies. E-Polymers. 2005; 002: 1-12

[26] Holland R, Eernisse EP. Accurate measurement of coefficients in a ferroelectric ceramic. IEEE Transactions on Sonics and Ultrasonics. 1969;SU16(4):173-184.

[27] Herbert JM. Ceramic dielectrics and capacitors. New York, N.Y. : Gordon & Breach; 1985.

[28] Malecki J, Hilczer B. Dielectric behavior of polymers and composites. In: DasGupta DK, editor. Ferroelectric Polymers and Ceramic-Polymer Composites, vol. 92-93 Stafa-Zurich: Trans Tech Publications Ltd; 1994. p. 181-215.

[29] Ma DL, Hugener TA, Siegel RW, Christerson A, Martensson E, Onneby C, et al. Influence of nanoparticle surface modification on the electrical behaviour of polyethylene nanocomposites. Nanotechnology. 2005;16(6):724-731.

[30] Vanturnhout J. Thermally stimulated discharge of electrets. Topics in Applied Physics. 1987;33:81-215.

Figures

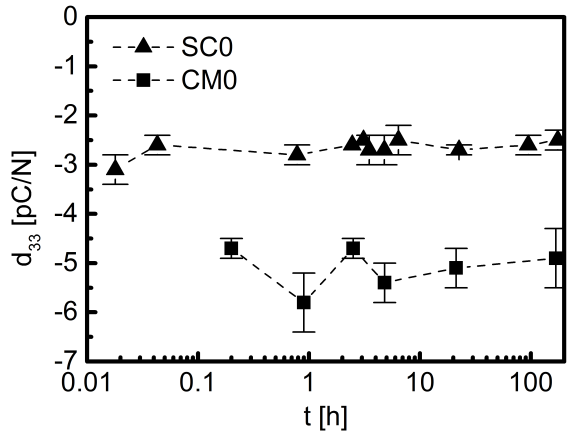

Fig.1. Piezoelectric coefficients of solvent cast and compression molded P(VDF-TrFE) films as a function of time (poling field: 100 kV/cm).

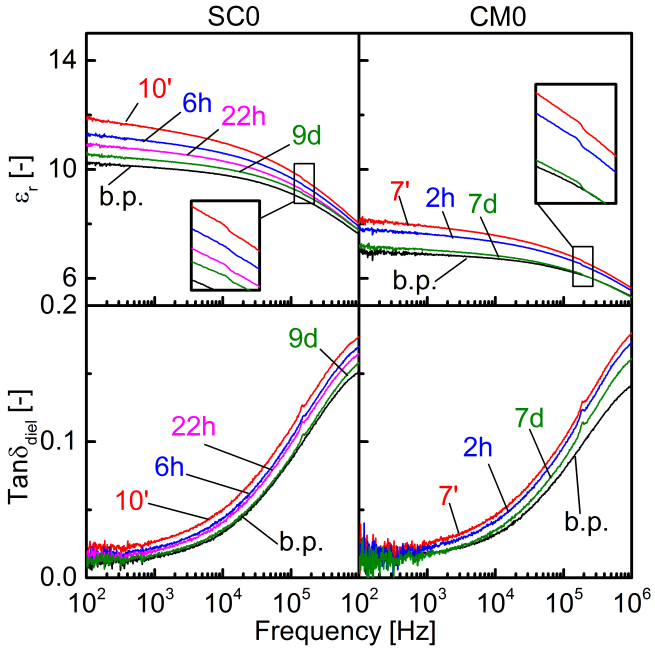

Fig. 2. Relative permittivity (ε_r) and dielectric loss tangent (tanδ_{diel}) of solvent cast (SC0) and compression molded (CM0) P(VDF-TrFE) before poling (b.p.) and in time after poling (elapsed time indicated for each curve). Resonance peaks enlarged in insets.

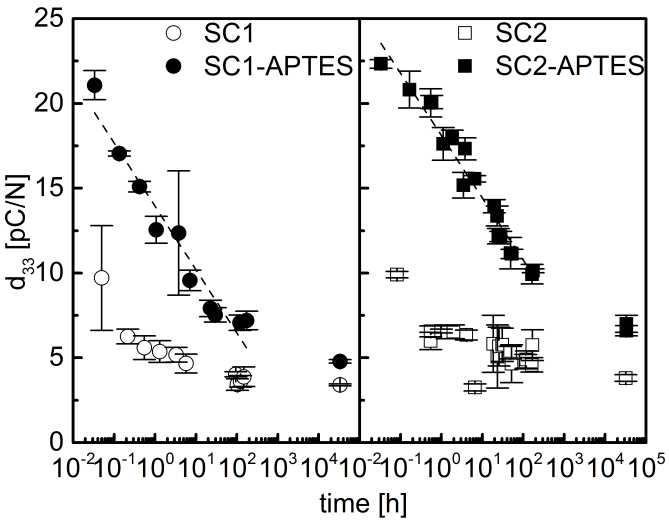

Fig. 3. Evolution of the piezoelectric coefficient d_{33} of SC composites with time from poling, and fitting of the data with equation 1 (dashed lines).

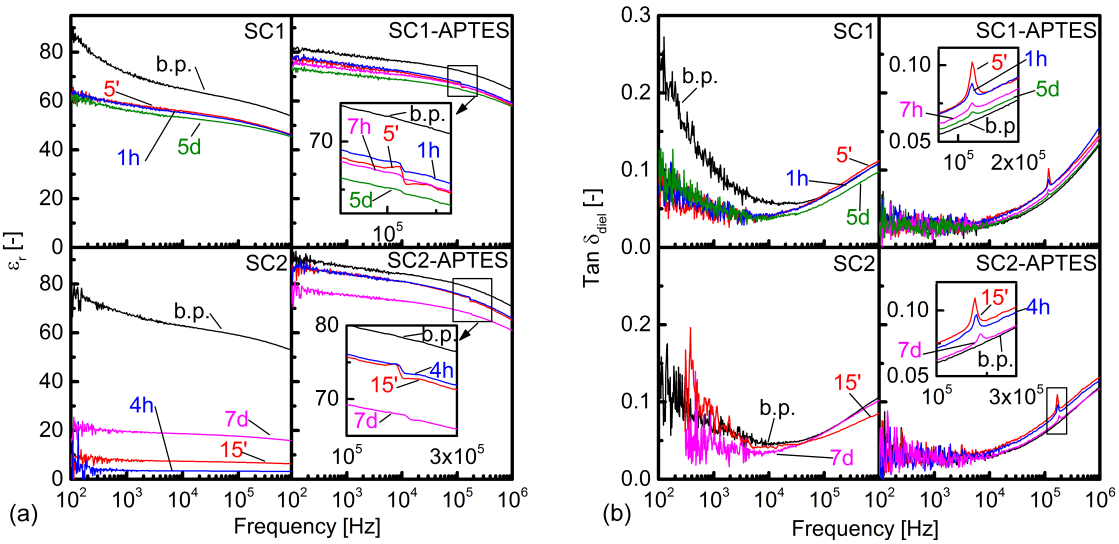

Fig. 4. (a) Relative permittivity (ε_r) and (b) dielectric loss tangent (Tanδ_{diel}) of SC composites before poling (b.p.), and after poling (elapsed time indicated for each curve). Resonance peaks enlarged in insets when clearly identified.

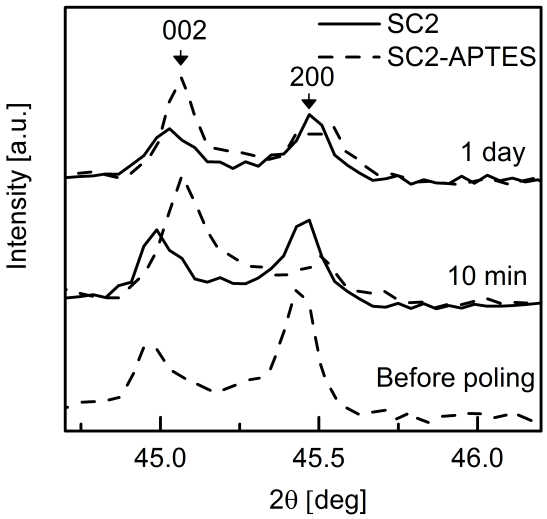

Fig. 5. X-ray diffraction patterns of SC composites containing pristine and APTES treated BT2

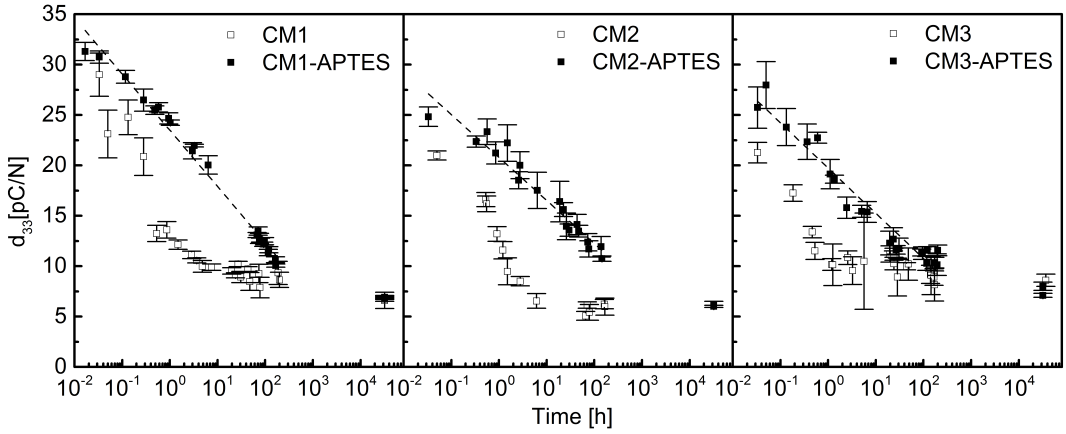

Fig. 6. Evolution of the piezoelectric coefficient d_{33} of CM composites with time from poling, and fitting of the data with equation 1 (dashed lines).

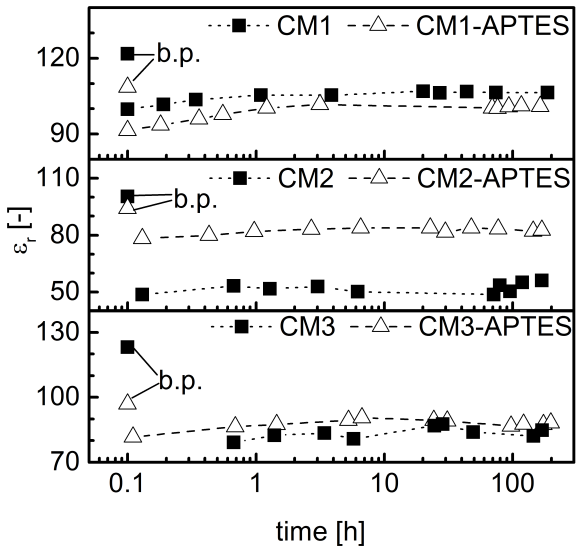

Fig. 7. Relative permittivity ε_r (measured at $5x10^4$ Hz) of CM composites before poling (b.p.) and as a function of time after poling.

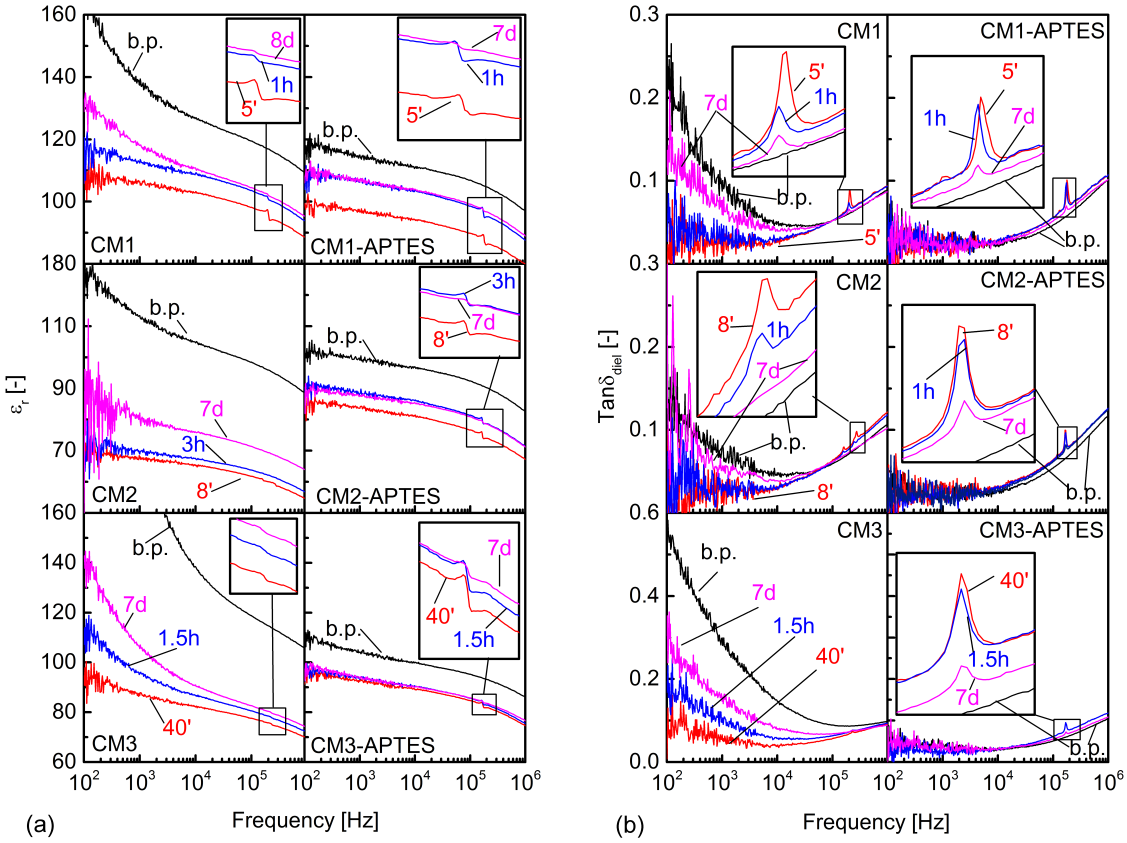

Fig. 8. (a) Relative permittivity (ε_r) and (b) dielectric loss tangent (Tanδ_{diel}) of CM composites before poling (b.p.), and after poling (elapsed time indicated for each curve). Resonance peaks enlarged in insets when clearly identified.

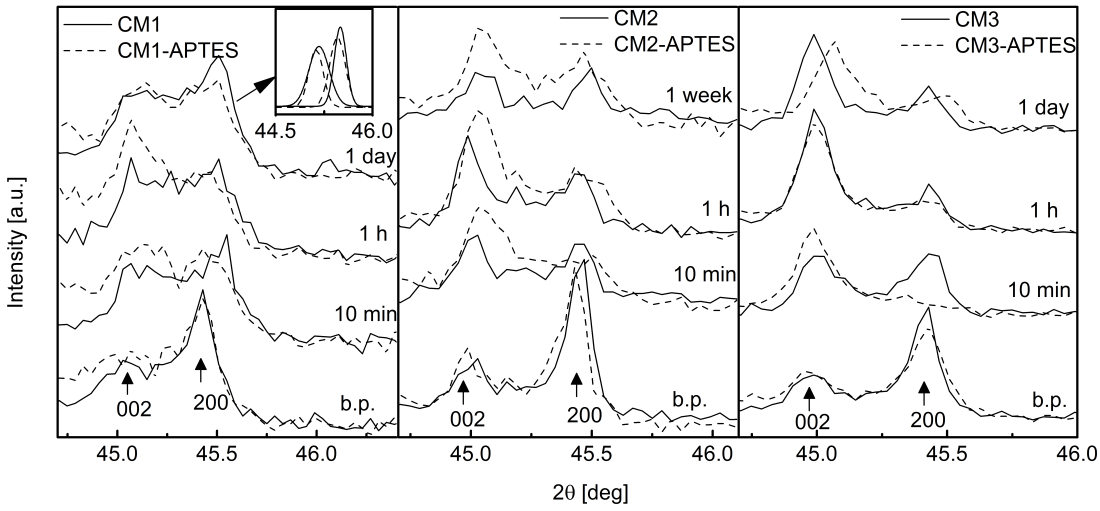

Fig.9. XRD patterns of CM composites, before poling (b.p.) and during time after poling (elapsed time indicated for each curve). The inset shows as example the peak fitting for CM1 and CM1-APTES, one day after poling.